Immobilized Chemoattractant Peptides Mediate Adhesion and Distinct Calcium-Dependent Cell Signaling in Human Neutrophils

Jonas Wetterö,*,† Tobias Hellerstedt,‡ Patrik Nygren,‡ Klas Broo,§ Daniel Aili,‡ Bo Liedberg,‡ and Karl-Eric Magnusson||

Rheumatology/AIR, Department of Clinical and Experimental Medicine, Linköping University, Linköping, Sweden, Division of Molecular Physics, Department of Physics, Biology and Chemistry, Linköping University, Linköping, Sweden, Occupational and Environmental Medicine, Sahlgrenska University Hospital, Göteborg University, Göteborg, Sweden, and Medical Microbiology, Department of Clinical and Experimental Medicine, Linköping University, Linköping, Sweden

Received November 9, 2007. Revised Manuscript Received April 11, 2008

Chemotaxis is the stimulated directional migration of cells in response to chemotactic factors, manifested for instance during leukocyte interaction with chemoattractants in inflammation. The *N*-formyl-Met-Leu-Phe (fMLF) bacterial peptide family is particularly potent in attracting and activating neutrophilic granulocytes. To accomplish defined circumstances for recruitment and activation of cells, we fabricated semitransparent gold-coated glass coverslips functionalized with chemoattractant fMLF receptor peptide agonist analogues. Peptides based on a common leading four-amino-acid sequence Gly-Gly-Gly-Cys were thus coupled to two potent fMLF receptor agonists, *N*-formyl-Tyr-Nle-Phe-Leu-Nle-Gly-Gly-Gly-Cys and *N*-formyl-Met-Leu-Phe-Gly-Gly-Gly-Cys, and a formylated control peptide, *N*-formyl-Gly-Gly-Gly-Cys. They were anchored via the SH group of Cys either directly to the gold surface or a mixed self-assembled monolayer composed of maleimide- and hydroxyl-terminated oligo(ethylene glycol) alkyldisulfides. The overall peptide immobilization procedure was characterized with ellipsometry, contact angle measurement, and infrared spectroscopy. When exposed to granulocytes, the agonist surface rapidly recruited neutrophils and the cells responded with extensive spreading and intracellular calcium transients within minutes. The reference peptide generated no such activation, and the cells maintained a more spherical morphology, suggesting that we have been able to immobilize chemoattractant receptor agonist peptides with retained bioactivity. This is a crucial step in designing surfaces with specific effects on cellular behavior.

Introduction

Chemotaxis plays a major role in inflammation, i.e., during recruitment of circulating leukocytes from the blood vessel lumen to the site of damaged tissue or infection.[1−3] It is thus desirable to understand and eventually control this intricately regulated directed cellular migration toward a gradient of stimuli in a number of diseases with an inflammatory component, for example, rheumatoid diseases, cancer, and atheriosclerosis, and also in wound healing. Chemoattractants comprise a multitude of stimuli that range from endogenous cytokines (chemokines), complement activation products, and lipid metabolites to exogenous molecules like the bacterial formyl-methionyl-leucyl-phenylalanine (fMLF or fMLP) peptide family. Locomotion is mediated via activation of serpentine (seven transmembrane, 7 TM) receptors, thereby triggering a phospholipase C-dependent transient cytosolic calcium mobilization and activation of protein kinase C. The bactericidal neutrophilic granulocytes (neutrophils) are highly motile upon fMLF stimulation, which triggers both chemotaxis and calcium-dependent oxidative metabolism.[4−7] Neutrophils express at least two G-protein receptors to fMLF, a high affinity formyl peptide receptor (FPR) and a low affinity formyl peptide receptor-like 1 (FPRL1).[8,9] The receptors are normally evenly distributed in the plasma membrane, but upon stimulation two functional receptor subpopulations accumulate in regions involved in motility.[10,11] Upon arrival to the tissue, these cells aim at eliminating pathogens by engulfment (phagocytosis) and/or by release of stored cytotoxic substances, e.g., hydrolytic enzymes and reactive oxygen species generated via the NADPH oxidase.

Despite that several experimental models to study leukocyte chemotaxis have been around for decades, as recently reviewed comprehensively,[12,13] a detailed understanding of chemoattractant receptor signaling and its complex dynamic interplay with cell adhesion molecules (selectins, integrins, and the

* Corresponding author, jonwe@imk.liu.se.
† Rheumatology/AIR, Department of Clinical and Experimental Medicine, Linköping University.
‡ Division of Molecular Physics, Department of Physics, Biology and Chemistry, Linköping University.
§ Occupational and Environmental Medicine, Sahlgrenska University Hospital, Göteborg University.
|| Medical Microbiology, Department of Clinical and Experimental Medicine, Linköping University.

(1) Ley, K.; Laudanna, C.; Cybulsky, M. I.; Nourshargh, S. *Nat. Rev. Immunol.* **2007**, *7*(9), 678–89.
(2) Uhing, J. R.; Snyderman, R. Chemoattractant stimulus-response coupling. In *Inflammation: Basic principles and clinical correlates*, 3rd ed.; Gallin, J. I., Snyderman, R., Eds.; Lippincott Williams & Wilkins: Philadelphia, 1999; pp 607−626.
(3) Simon, S. I.; Green, C. E. *Annu. Rev. Biomed. Eng.* **2005**, *7*, 151–185.
(4) Showell, H. J.; Freer, R. J.; Zigmond, S. H.; Schiffmann, E.; Aswanikumar, S.; Corcoran, B.; Becker, E. L. *J. Exp. Med.* **1976**, *143*(5), 1154–1169.
(5) Niedel, J.; Wilkinson, S.; Cuatrecasas, P. *J. Biol. Chem.* **1979**, *254*(21), 10700-6.
(6) Panaro, M. A.; Mitolo, V. *Immunopharmacol. Immunotoxicol.* **1999**, *21*(3), 397–419.
(7) Remes, J. J.; Petaja-Repo, U. E.; Tuukkanen, K. J.; Rajaniemi, H. J. *Exp. Cell Res.* **1993**, *209*(1), 26–32.
(8) Selvatici, R.; Falzarano, S.; Mollica, A.; Spisani, S. *Eur. J. Pharmacol.* **2006**, *534*(1−3), 1–11.
(9) Fu, H.; Karlsson, J.; Bylund, J.; Movitz, C.; Karlsson, A.; Dahlgren, C. *J Leukoc Biol* **2006**, *79*(2), 247–256.
(10) Johansson, B.; Wymann, M. P.; Holmgren-Peterson, K.; Magnusson, K. E. *J. Cell Biol.* **1993**, *121*(6), 1281–1289.
(11) Loitto, V. M.; Rasmusson, B.; Magnusson, K. E. *J. Leukocyte Biol.* **2001**, *69*(5), 762–771.
(12) Entschladen, F.; Drell, T. L. t.; Lang, K.; Masur, K.; Palm, D.; Bastian, P.; Niggemann, B.; Zaenker, K. S. *Exp. Cell Res.* **2005**, *307*(2), 418–426.
(13) Frow, E. K.; Reckless, J.; Grainger, D. J. *Med. Res. Rev.* **2004**, *24*(3), 276–298.

10.1021/la703502y CCC: $40.75
Published on Web 05/29/2008

immunoglobulin superfamily) and other immunological receptors is not available. Established methods employ measurement of a leading front of a population of cells and include two-compartment filter assays,[14,15] migration under cell-impermeable agarose,[16,17] cell-permeable gels of structural extracellular matrix proteins,[18] and different types of microscopy chambers.[19,20] Some experimental platforms are optimized for combination with cellular imaging and individual cell tracking in three dimensions.[12,13,21,22] Still some limitations remain, for example, compatibility issues and lack of a detailed spatial and temporal control of chemoattractant distribution or failure to provide a well-defined mixture of different stimuli. Furthermore, stimulation of either FPR or FPRL-1 triggers functionally similar oxidative activation patterns in neutrophils, and assaying the ratio between the respiratory burst triggered by specific agonists could be a promising tool in several applications.[23] Chemoattractant peptides are often anticipated to exert their actions only as soluble molecules, but they do also attach to the substratum. This was early on observed in vitro for fMLF in the under-agarose chemotaxis system displaying a gradient of surface-bound chemoattractants,[17] and chemokines can be localized by specific and nonspecific binding to glycosaminoglycans and thus proteoglycans on the surfaces of cells or in the extracellular matrix.[24–27] Hence it is desirable to be able to attach an active peptide or combinations of peptides to surfaces, thereby facilitating gradient design and enabling restimulation of the cells with other agonists and combination with established and emerging techniques. Immobilization of chemoattractants on supporting substrates offer a precise and controlled alternative to humoral stimulation and could enhance the current understanding of inflammation and tissue engineering. This is also applicable to biosensor design where cells could be recruited to a specific site. Related but based on different concepts are provided by the integrin receptor RGD adhesion motifs at interfaces to promote firm cell−surface interactions in biomaterials,[28] the careful simultaneous design of both surface chemistry and topology of to control mammalian cell behavior at imaging-compatible interfaces,[29,30] and the microparticle-based slow-release models for chemoattractants.[31] We have aimed at an immobilization strategy allowing imaging of de novo synthesized potent fMLF receptor peptide agonist analogues; *N*-formyl-Met-Leu-Phe and *N*-formyl-Tyr-Nle-Phe-Leu-Nle modified with a spacer tail Gly-Gly-Gly and a C-terminal cysteine that permit site-specific attachment via thiol coupling to gold or a maleimide-containing self-assembled monolayer (SAM). A N-terminal formylated Gly-Gly-Gly-Cys peptide was used as a reference peptide. The use of a maleimide-containing SAM[32,33] (Figure 1) offers molecular flexibility, adjustable peptide surface concentration, controlled peptide−surface vertical distance, and, most importantly, efficient shielding of cells from directly interacting with the supporting gold substrate. The importance of such a barrier layer is clearly demonstrated and suggests that the two-step maleimide−peptide immobilization process used offers a convenient route for the generation of a biologically active fMLF receptor peptide surface compatible with cellular imaging.

Results and Discussion

Biological Activity of Peptides. The two receptor agonist motifs were designed to be potent activators of the neutrophil chemotaxis, cytosolic calcium and the respiratory burst. However, in order to ascertain that their biological activity maintained after addition of the Gly-Gly-Gly-Cys sequence, submicromolar concentrations of the synthesized peptide analogues were initially screened for neutrophil NADPH oxidase activation capacity (Figure 2A). Both agonist analogues yielded rapid generation of reactive oxygen species in a similar fashion as the original agonists (lacking the Gly-Gly-Gly-Cys motif). The short formylated control peptide showed no apparent sign of triggering neutrophil bactericidal activity.

Ratio Imaging. Chemoattractants trigger calcium transients, and fluorescence ratio imaging[34,35] was thus chosen to study fMLF activation of neutrophils on substrates. The peptide immobilization and characterization protocol required a gold support, and hence it was necessary to use gold films also during cell activation experiments. Unfortunately, direct application of single excitation wavelength fluorescence microscopy in live cellular imaging on nontransparent reflective metal films introduces several challenges. These include primarily general distortion and rapid decay in emission because of extensive light reflections, particulary in the absence of antifading agents, but there are also difficulties in confirming the true origin of emission. By fabricating semitransparent coverslips, it was possible to use simultaneous bright-field imaging to ascertain fluorescence emanating from the cytosol of individual cells. When using fura-2, a fluorophore that display opposite optical responses at two different excitation wavelengths, it is possible to work with the ratio and thereby obtain a more reliable stable baseline and a high dynamic range, relatively independent of various confounders, for example, morphology of the cells and noise. Accordingly, soluble fMLF receptor agonists were found to trigger cytosolic calcium transients in *individual* neutrophils when ratio imaging was performed through the semitransparent gold. This is clearly evident in Figure 2B where we show typical calcium transients in five different cells. These signals precede the respiratory burst seen in Figure 2A.

(14) Boyden, S. *J. Exp. Med.* **1962**, *115*, 453–466.
(15) Zigmond, S. H.; Hirsch, J. G. *J. Exp. Med.* **1973**, *137*(2), 387–410.
(16) Issekutz, A.; Ripley, M.; Bhimji, S. *J. Immunol. Methods* **1983**, *59*(1), 19–28.
(17) Dahlgren, C.; Magnusson, K. E.; Sundqvist, T. *J. Immunol. Methods* **1984**, *75*(1), 23–29.
(18) Islam, L. N.; McKay, I. C.; Wilkinson, P. C. *J. Immunol. Methods* **1985**, *85*(1), 137–151.
(19) Zicha, D.; Dunn, G. A.; Brown, A. F. *J. Cell Sci.* **1991**, *99*(Pt 4), 769–775.
(20) Zigmond, S. H. *J. Cell Biol.* **1977**, *75*(2 Pt 1), 606–616.
(21) Moghe, P. V.; Nelson, R. D.; Tranquillo, R. T. *J. Immunol. Methods* **1995**, *180*(2), 193–211.
(22) Soon, L.; Braet, F.; Condeelis, J. *Microsc. Res. Tech.* **2007**, *70*(3), 252–257.
(23) Fu, H.; Karlsson, J.; Björkman, L.; Stenfeldt, A. L.; Karlsson, A.; Bylund, J.; Dahlgren, C. *J. Immunol. Methods* **2008**, *331*(1−2), 50–58.
(24) Johnson, Z.; Proudfoot, A. E.; Handel, T. M. *Cytokine Growth Factor Rev.* **2005**, *16*(6), 625–636.
(25) Kuschert, G. S.; Coulin, F.; Power, C. A.; Proudfoot, A. E.; Hubbard, R. E.; Hoogewerf, A. J.; Wells, T. N. *Biochemistry* **1999**, *38*(39), 12959–12968.
(26) Middleton, J.; Neil, S.; Wintle, J.; Clark-Lewis, I.; Moore, H.; Lam, C.; Auer, M.; Hub, E.; Rot, A. *Cell* **1997**, *91*(3), 385–395.
(27) Witt, D. P.; Lander, A. D. *Curr. Biol.* **1994**, *4*(5), 394–400.
(28) Hersel, U.; Dahmen, C.; Kessler, H. *Biomaterials* **2003**, *24*(24), 4385–4415.
(29) Brock, A.; Chang, E.; Ho, C.; LeDuc, P.; Jiang, X.; Whitesides, G.; Ingber, D. E. *Langmuir* **2003**, *19*, 1611–1617.
(30) Mrksich, M.; Chen, C. S.; Xia, Y.; Dike, L. E.; Ingber, D. E.; Whitesides, G. M. *Proc. Natl. Acad. Sci. U.S.A.* **1996**, *93*(20), 10775–10778.
(31) Zhao, X.; Jain, S.; Benjamin Larman, H.; Gonzalez, S.; Irvine, D. J. *Biomaterials* **2005**, *26*(24), 5048–5063.
(32) Ekeroth, J. Phosphorylated monomolecular layers. Design, synthesis, characterization and application. Linköping Studies in Science and Technology. Dissertation No. 764. Linköping University, Linköping, Sweden, 2002.
(33) Houseman, B. T.; Gawalt, E. S.; Mrksich, M. *Langmuir* **2003**, *19*(5), 1522–1531.
(34) Grynkiewicz, G.; Poenie, M.; Tsien, R. Y. *J. Biol. Chem.* **1985**, *260*(6), 3440–3450.
(35) Tsien, R. Y.; Rink, T. J.; Poenie, M. *Cell Calcium* **1985**, *6*(1−2), 145–157.

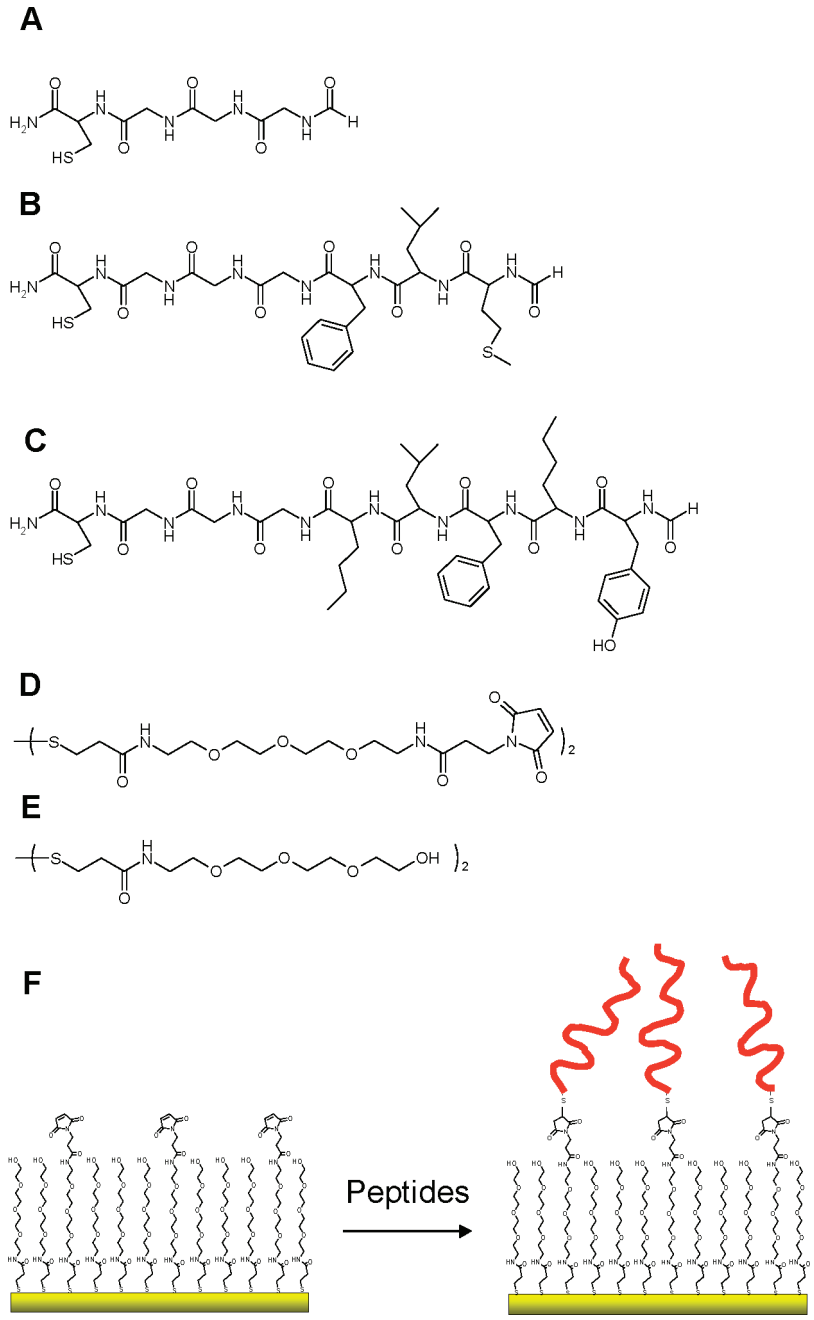

Figure 1. Control peptide *N*-formyl-Gly-Gly-Gly-Cys (A) and the two fMLF receptor agonist analogues *N*-formyl-Met-Leu-Phe-Gly-Gly-Gly-Cys (B) and *N*-formyl-Tyr-Nle-Phe-Leu-Nle-Gly-Gly-Gly-Cys (C), synthesized with solid phase peptide synthesis. Chemical structures of the maleimide- (D) and hydroxyl-terminated EG_4 disulfides (E) used to form the SAMs onto which the synthesized peptides were immobilized (as described in (F).

Thickness and Wettability of Peptide Layers and SAMs. The control and agonist peptides were site-specifically immobilized directly to gold by employing thiol coupling via the C-terminal cysteine, resulting in ellipsometric layer thicknesses between ~12 and 20 Å and contact angles of 12−72° (Supporting Information S1). Unfortunately, this immobilization protocol yielded layers of the control peptide and the two agonist analogues for which the subsequent neutrophil responses were similar to those obtained for bare gold (data not shown). These observations clearly suggested that the neutrophils can sense the underlying substrate and that the vertical distance between the surface and the peptides has to be increased by forming a dense barrier SAM on the gold surface. The thicknesses of such barrier SAMs composed of hydroxyl- and maleimide-terminated EG_4 disulfides[32,33] were found to be ~14 and ~19 Å, depending on the relative composition of 10% or 100% of maleimide-termination, respectively. Subsequent formation of peptide layers on top of the barrier SAMs revealed incremental thickness changes Δd of about 1−2 and 5−15 Å for surfaces with 10% and 100% maleimide-termination, respectively (Table 1). The increases in contact angle after peptide agonist immobilization were in concert with the ellipsometric thicknesses and the contact angles obtained for the pure peptide layers. Thus, the *N*-formyl-Gly-Gly-Gly-Cys is a hydrophilic peptide, whereas both agonists tend to be more hydrophobic, the long *N*-formyl-Tyr-Nle-Phe-Leu-Nle-Gly-Gly-Gly-Cys in particular.

Infrared Spectroscopy. The isotropic IR transmission spectra of the synthesized peptides dispersed in KBr and pressed into pellets are shown in Figure 3. Considerable effort has been devoted to studies aimed at finding correlations between the amide I peak

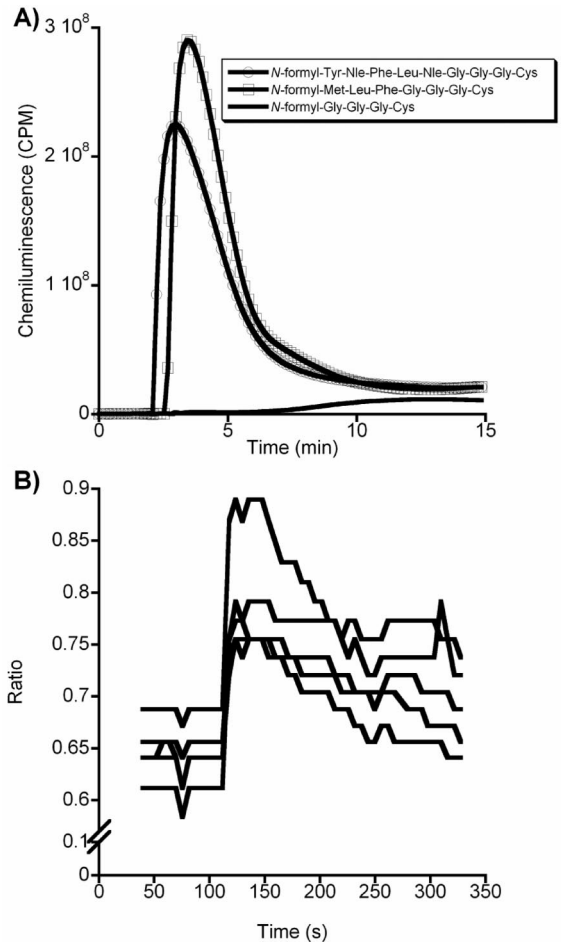

Figure 2. (A) Representative temporal resolution of the generation of reactive oxygen species following stimulation of 1×10^6 neutrophils with 100 nM in a six-channel Biolumat. Experiments performed in KRG at 37 °C in the presence of 56.4 μM luminol and 4U/mL horseradish peroxidase. (CPM = counts per min.) (B) The ratio change (increase in cytosolic calcium ion concentration) in five individual neutrophils poststimulation with 100 nM *N*-formyl-Tyr-Nle-Phe-Leu-Nle-Gly-Gly-Gly-Cys, imaged through gold-coated coverslips. Neutrophils were preloaded with fura-2 and excited at 340 and 380 nm emission recorded at 510 nm, with 10 ratio images proportional to the ion concentration recorded for every minute.

position and the secondary structure of the polypeptide backbone, and as a rule of thumb, polypeptides exhibiting the antiparallel β-sheet conformation absorb in the ranges ~1675−1695 and ~1625−1640 cm^{-1}, the α-helical ~1648−1660 cm^{-1}, and the unordered state ~1646−1658 cm^{-1}.[36] For the short control peptide at least three different amide I peaks could be seen in the fingerprint region of the isotropic IR spectrum (Figure 3A). The amide I peak frequencies range from 1634 to 1689 cm^{-1} with a dominating feature at 1634 cm^{-1}, indicating, at first glance and according to the guide lines above, that the peptide backbone adopts the β-sheet conformation. For the long agonist (Figure 3B) a single peak was seen at 1650 cm^{-1}, whereas two amide I peaks were found in the range 1636−1654 cm^{-1} for the short agonist (Figure 3C). Although the peptides displayed amide I peaks in the regions expected for α-helical and β-sheet conformations, it is doubtful whether they can be attributed to extended segments of such conformations considering the short length of the peptides. It is more likely that the polypeptide backbones consist of significant amounts of unordered segments, an assumption supported by the Chou-Fasman rules.[37,38] We thus conclude that the infrared spectra of the peptides display a varying distribution of amide I peaks, which most likely reflects the complicated interplay between intra- and interchain interactions occurring in the crystalline state. The amide II peak, which is less sensitive to polypeptide chain conformation, could be found at about 1546 cm^{-1} for the control and the shorter agonist peptides, respectively, but had shifted to 1517−1536 cm^{-1} (two peaks) for the long agonist. The 1517 cm^{-1} peak is attributed to the tyrosine residue, which is present only in that spectrum of long agonist (Figure 3B). Moreover, the amide III peak appeared as a broad feature near 1235 cm^{-1} in all peptide spectra, and $CH_{2,3}$ bending modes from the amino acid side chains in the range 1370−1470 cm^{-1}. Peaks were also seen near 3295 cm^{-1} and in the range 2850−3000 cm^{-1} and they are assigned to NH stretching (amide A) and $CH_{2,3}$ stretching modes, respectively (not shown).

The fine details seen in the RA spectra of the various peptide layers are dependent on the procedure used to obtain representative spectra. For instance, the spectrum in Figure 4A is the sum of the spectra of the maleimide SAM and the attached peptide overlayer, here represented by the long agonist. In order to obtain a spectrum of the peptide overlayer (C), it is necessary to subtract the maleimide SAM spectrum in Figure 4B from that in Figure 4A. This prodecure unfortunately introduced distortions in the amide I region, because of the C═O peak of the maleimide residue which absorbs strongly near 1700 cm^{-1}. When the peptide reacts with the maleimide residue, the electronic structure of the ring is affected leading to a small downward shift of the C═O strecthing frequency. This shift will show up as a derivative-like peak (∗) in the difference spectrum Figure 4C. The new peak interferes with the intensity distribution in the amide I region and makes the use of the amide I peak as diagnostic tool for predicting the secondary structure of the polypeptide backbone uncertain. Note, however, that the effect is only visible in spectra of SAMs with 100% maleimide termination, that is, for SAMs with a high amount of immobilized peptide.

Figure 5 (panels I, II, III) shows representative RA spectra of the three peptides immobilized either directly to gold (A) or via the SAMs with 100% (B) and 10% (C) maleimide termination, respectively. The intensities of the amide I, II, and III peaks were consistently higher in the spectra of the peptides directly attached to gold and decreased with decreasing maleimide termination, in full agreement with the ellipsometric findings (Table 1 and Supporting Information S1). The positions of the amide I peaks were all shifted to higher frequencies in the RA spectra, as compared to the KBr spectra (see Figures 5 and 3). The magnitude of the shift varied but appeared to fall in the range 25−50 cm^{-1}. Such blue shifts have been observed before, and they have been attributed to conformational changes in the peptide backbone and/or to optical effects.[39] The optical effects occur because of the strong dispersion in the refractive index near the absorption maximum and appear in reflection spectra recorded in the RA mode as well as in the attenuated total reflection (ATR) mode. To separate the two contributions to the blue shifts from each other requires tedious spectral simulations,[40,41] and this is beyond the scope of the present paper.

It was also observed in Figure 5 that the relative intensities

(36) Jackson, M.; Mantsch, H. H. *Crit. Rev. Biochem. Mol. Biol.* **1995**, *30*(2), 95–120.
(37) Levitt, M. *Biochemistry* **1978**, *17*(20), 4277–4285.
(38) Chou, P. Y.; Fasman, G. D. *Biochemistry* **1974**, *13*(2), 222–245.
(39) Liedberg, B.; Ivarsson, B.; Hegg, P. O.; Lundström, I. *J. Colloid Interface Sci.* **1986**, (114), 386.
(40) Ihs, A.; Liedberg, B.; Uvdal, K.; Törnkvist, C.; Bodö, P.; Lundström, I. *J. Colloid Interface Sci.* **1990**, (140), 192.
(41) Parikh, A. N.; Allara, D. L. *J. Chem. Phys.* **1992**, (96), 927.

Table 1. Incremental Layer Thickness Δd of SAMs of Hydroxyl- and Maleimide-Terminated EG_4 Disulfides upon Attachment of the Three Peptides[a]

peptide	10% malemide in SAM[b]		100% malemide in SAM[b]	
	Δd (Å)[c]	θ_s (deg)	Δd (Å)[c]	θ_s (deg)
N-formyl-Gly-Gly-Gly-Cys	0.6 ± 0.6	26 ± 2	5.2 ± 0.9	15 ± 2
N-formyl-Met-Leu-Phe-Gly-Gly-Gly-Cys	1.0 ± 0.6	34 ± 1	6.5 ± 1.7	51 ± 4
N-formyl-Tyr-Nle-Phe-Leu-Nle-Gly-Gly-Gly-Cys	1.7 ± 0.6	37 ± 1	14.7 ± 3.3	68 ± 6

[a] Corresponding static contact angles are also shown. [b] The ellipsometric thickness is 13.8 ± 1.2 Å and the static contact angle is 32 ± 2° for the 10% malemide SAM, and 18.7 ± 1.2 Å and 41 ± 2° for the 100% malemide SAM, respectively. [c] The standard deviations were obtained from measurements at five different points on each sample, and the number of samples was at least five for each peptide coating.

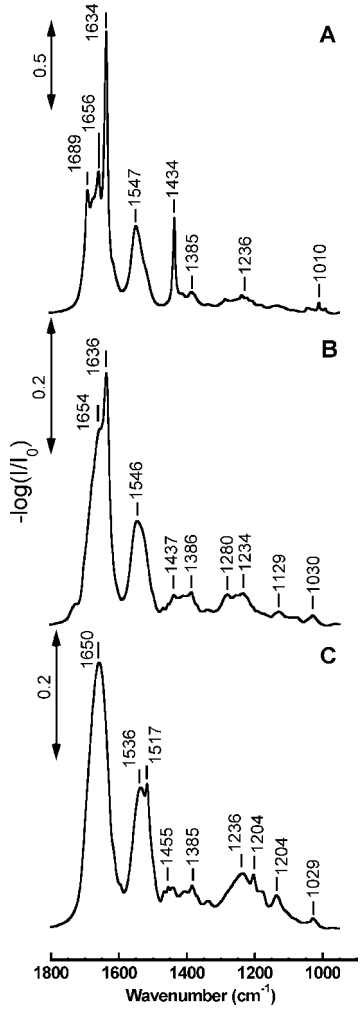

Figure 3. Isotropic IR spectra for (A) the short formylated control peptide, (B) the short agonist, and (C) the long agonist.

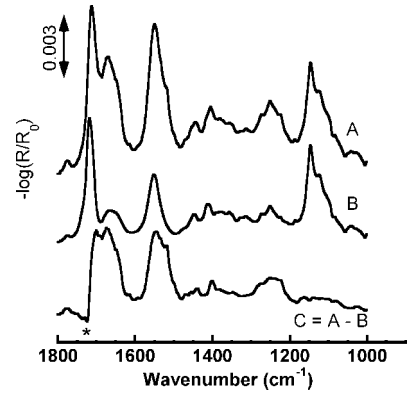

Figure 4. Procedure used where the infrared RA spectrum of a surface coated with 100% of maleimide-terminated EG_4 disulfides (B) is subtracted from the RA spectrum obtained when a layer of the long agonist is coupled to the maleimide-terminated EG4 disulfides (A), to obtain the spectrum for the agonist peptide layer only (C). As seen in spectrum C, some artifacts may arise due to shift in wavenumbers upon binding of the agonist to the SAM of maleimides.

between the amide I and II peaks differed in the crystalline and adsorbed states. The A_I:A_{II} intensities in the crystalline state varied typically between 2:1 to 3:1, whereas the same values in the adsorbed state were around 1.5:1 for the control peptide and near 1:1 for the long and short peptides. The relative increase in the amide II intensity, seen in the RA spectra of the adsorbed layers, is most likely due to a preferential alignment of the transition dipole moment of the amide II mode (|| to the C−N bond) with respect to the surface normal,[42] whereas the corresponding transition moment of the amide I mode (⊥ to the C═O bond) tends to align in an orientation parallel to the underlying metal surface (perpendicular to the surface normal). These intensity observations suggest that the peptides formed extended assemblies with their chain axes preferentially aligned perpendicularly to the surface. We are, however, a little bit hesitant to attribute the observed positions/intensities of the amide I and II peaks to a particular chain conformation because of the inferring contribution origination from optical effects.

Neutrophil−Matrix Interactions. Fura-2-loaded neutrophils were exposed to the peptide−SAMs, and Ca^{2+}-signaling was assessed by fluorescence ratio imaging. Cells were given time to sediment onto the SAMs, and changes in cytosolic calcium were then monitored for 10−15 min. Parallel bright-field imaging revealed a rapid association and cell spreading during the interaction with the long agonist, for both 10% and 100% maleimide terminations (Supporting Information, S2 and S3). Surface cell attachment was very modest on the formylated control peptide SAM. Only scattered cells adhered with maintained spherical morphology. The long agonist−SAM triggered a distinct cytosolic calcium transient in the neutrophils, peaking within 1−2 min postadhesion (Figure 6 and Figure 7A). The magnitude and temporal resolution is similar to what is seen following humoral stimulation of neutrophils with the long agonist analogue (Figure 2B). For comparison, a subsequent secondary stimulation with soluble fMLF yielded a smaller cytosolic calcium mobilization at the long agonist surface (Figure 7B), indicating that the surface-triggered activation was a true FPR-mediated response. By contrast, the formylated control peptide yielded no such apparent cytosolic calcium increase in surface-associated cells (not shown). The poor adhesion onto the control surface made quantitative ratioing in individual cells over sustained times more difficult, since cells did not attach firm enough to remain in the observed microscopy view for more than a few minutes. Despite this, it was possible to record a short sequence on this control matrix where neutrophils were clearly shown to retain full calcium mobilization potential in response to a humoral

(42) Valiokas, R.; Svedhem, S.; Svensson, S. C. T.; Liedberg, B. *Langmuir* **1999**, (15), 3390.

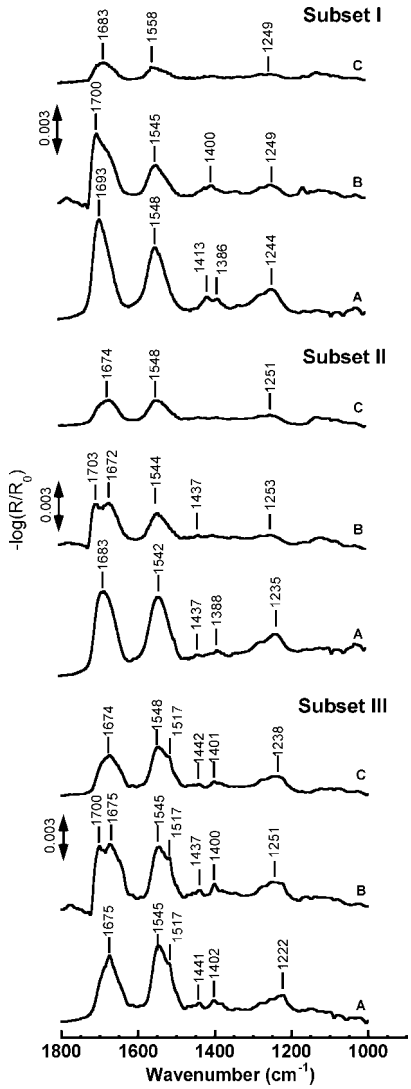

Figure 5. Infrared RA spectra obtained when immobilizing the formylated control peptide (Subset I) directly to gold-coated surfaces (A) and to mixed SAMs of maleimide- and hydroxyl-terminated EG_4 disulfides, with maleimide-termination of 10% (C) and 100% (B), respectively. Spectra obtained with similarly treated surfaces with (Subset II) the short agonist peptide and (Subset III) the long agonist.

stimulation with fMLF (Figure 7C). Furthermore, immediately upon soluble fMLF-stimulation bright-field imaging revealed that the neutrophils now tried to extend protrusions, yet remaining unsuccessful in acquiring a firm adhesion to the control substratum (not shown). Moreover, presence of fMLF in solution prior to adhesion of cells inhibited or delayed neutrophil spreading on the agonist substratum (Supporting Information, S3). This supports the suggestion of FPR-mediated activation at the agonist surface and, importantly, a very low nonspecific activation by the shielding maleimide−SAM. This is an important observation, since in line with previous work in our laboratory,[43] the ratio imaging also showed that bare gold surfaces instead form a rather hostile environment for blood cells such as neutrophils and that fMLF−peptide analogues being immobilized without the SAMs failed in triggering apparent calcium activation (not shown). The latter was most likely because of the nonspecific nature of the preactivation mediated by bare gold and surface contact per se, probably engaging a multitude of cell adhesion receptors (including the integrins).

Fixation of cells subsequent to ratio imaging sessions, followed by Alexa488−phallacidin staining and fluorescence microscopy evaluation of the filamentous actin cytoskeleton confirmed the real-time bright-field image observations. The chemoattractant peptide SAM (Figure 8A) rapidly recruited neutrophils to near confluency, with good spreading, supporting a good bioavailability of the chemoattractant peptide with an intact cell recruiting capacity. In this regard, it is possible to consider fMLF- and nonstimulated neutrophils almost as two separate cell populations. Depending on the dose, neutrophil interaction with the chemoattractant will not only affect FPR/FPRL-1 binding and receptor distribrution but also regulate the expression of a number of true cell adhesion receptors, e.g., integrins, with putative specific and nonspecific binding capacities to a multitude of biological and artificial surfaces. In order to assess whether the adhesion at the agonist surface was mainly a FPR-mediated event, neutrophil FPRL-1 and a major adhesion integrin complement receptor type 3 (CR3, same as CD18/CD11b) were blocked prior to surface interactions via neutrophil preincubation with relatively high doses of FPRL-1 antagonist peptide WRWWWW or anti-CD11b monoclonal antibody LM2/1.6.11, respectively (Supporting Information, S2). For the short duration (10−15 min) of cell−surface interaction in the scope of the present study, these measures did not affect neutrophil adhesion, spreading, or filamentous actin distribution. In line with this, LM2/1.6.11 showed no effect on the calcium response triggered by the long agonist surface (not shown). On the contrary, the cell count was indeed lower on the formylated control peptide surface (Figure 8B) and morphology similar to what could be expected for any surface coated with a low-adhesive motif. Although, the local coverage in the selected area shown in Figure 8B is higher than the average microscope view, the cells maintained a spherical morphology typical for nonactivated neutrophils. Taken together, our observations clearly demonstrate that a spacer layer is an absolute prerequisite to avoid interfering interactions with the gold substrate. The OEG portion of the spacer also provides a biocompatibile environment for the interacting cells.

Neutrophil Interactions with Immobilized Chemoattractants during Inflammation. Facing the complexity of neutrophil recruitment, the application potential of designed chemoattractant surfaces is vast. It can help address a multitude of mechanisms at almost any stage of the process and with strong clinical bearings. It includes various blood and tissue cells, and it ranges from endothelial cell capture to paracellular or transcellular transmigration and migration of cells through the extracellular matrix.[1] Further insight is warranted on chemokine localization by chemokine binding to glycosaminoglycans,[24–27] pericellular coatings,[44] general and specific effects of coimmobilization with adhesive proteins, chemokine-triggered down-regulation of chemoattractant-stimulated migration,[45] immune complex and/or complement activation in the extracellular matrix,[46] or at interfaces between blood and the solid,[47,48] and for chemosensory

(43) Wetterö, J.; Askendal, A.; Tengvall, P.; Bengtsson, T. *J. Biomed. Mater. Res., Part A* **2003**, *66*(1), 162–175.
(44) Cohen, M.; Joester, D.; Geiger, B.; Addadi, L. *ChemBioChem* **2004**, *5*(10), 1393–1399.
(45) Lang, K.; Hatt, H.; Niggemann, B.; Zaenker, K. S.; Entschladen, F. *Scand. J. Immunol.* **2003**, *57*(4), 350–361.
(46) Sjöberg, A.; Önnerfjord, P.; Mörgelin, M.; Heinegård, D.; Blom, A. M. *J. Biol. Chem.* **2005**, *280*(37), 32301-8.
(47) Wetterö, J.; Askendal, A.; Bengtsson, T.; Tengvall, P. *Biomaterials* **2002**, *23*(4), 981–991.
(48) Andersson, J.; Ekdahl, K. N.; Lambris, J. D.; Nilsson, B. *Biomaterials* **2005**, *26*(13), 1477–1485.
(49) Chang, C. C.; Lieberman, S. M.; Moghe, P. V. *J. Mater. Sci. Mater. Med.* **2000**, *11*(6), 337–344.
(50) Chang, C. C.; Rosenson-Schloss, R. S.; Bhoj, T. D.; Moghe, P. V. *Biomaterials* **2000**, *21*(22), 2305–2313.

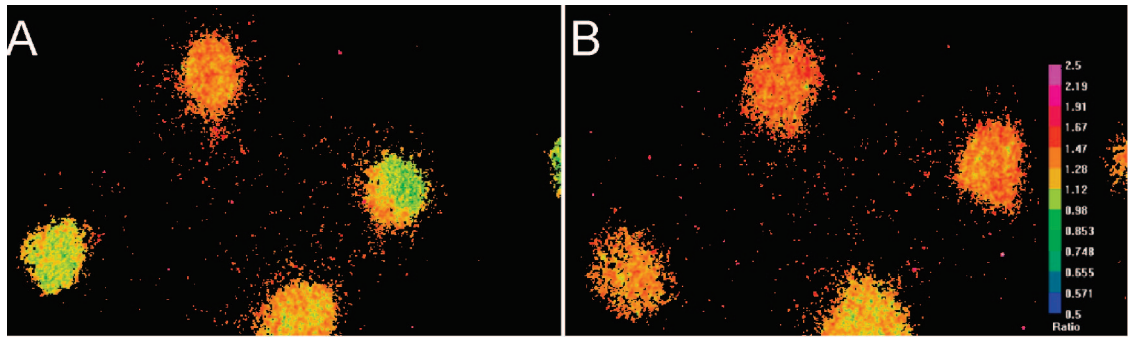

Figure 6. Increase in the concentration of cytosolic calcium during neutrophil interaction with a gold-coated coverslip functionalized with the long fMLF receptor agonist peptide (10% maleimide termination). Neutrophils were preloaded with calcium-binding probe fura-2. Adhering cells were alternately excited at 340 and 380 nm and emitted fluorescence recorded at 510 nm, yielding one ratio (340/380 nm) image proportional to the absolute ion concentration for every sixth second. The ratio in (A) is obtained immediately after settling of cells in the focal plane, and (B) is the ratio obtained 2 min later.

migration on biomaterials.[49,50]

In summary, the proposed immobilization protocol of fMLF receptor agonists yielded SAMs that trigger chemoattractant stimulation of human neutrophil granulocytes. Future experiments will assess the impact of this approach, using different ligand−receptor combinations, and involve peptides in mixed layers, gradients, and/or patterns, making more extensive studies on cell migration feasible.

Conclusions

We have demonstrated how two fMLF receptor peptide agonists may be designed to suit thiol coupling to semitransparent gold coverslips with retained ability to trigger neutrophil activation. By immobilization of the peptides to SAMs of maleimide- and hydroxyl-terminated and OEG containing alkyldisulfides on gold, it is possible prevent interfering interactions with the gold substrate and obtain fully functional peptide layers. The agonist triggers appropriate neutrophil activation after immobilization, as evidenced by calcium-dependent signaling and rapid association and spreading on the substrate. Thus, we believe that the employed approach can be further developed into an experimental platform for studies of cell adhesion and activation.

Experimental Section

Peptides. Two analogues (Figure 1A,B) to known fMLF receptor agonists, as well as one formylated control peptide (Figure 1C), were synthesized on 0.1−0.2 mmol scales using standard fluorenylmethoxycarbonyl (Fmoc) chemistry and *O*-(7-benzotriazole-1-yl)-1,1,3,3-tetramethyluronium tetrafluoroborate (TBTU, Alexis Biochemicals, Lausen, Switzerland) as the activating reagent on a Pioneer automated peptide synthesizer (Applied Biosystems, Foster City, CA). An Fmoc-PAL-PEG-PS resin (Applied Biosystems) was used as solid support, and amino acids (Calbiochem-Novabiochem AG, Laudelfingen, Switzerland) were added in 4-fold excess. For Cys the side chain was protected with trityl. The N-terminal of the peptides was formylated by adding diisopropylethylamine (DIPEA, Perseptive Biosystems, Framingham, MA) (1.5 equiv) in dichloromethane (DCM, Fluka Chemie AG, Buchs, Switzerland) to the resin followed by a mixture consisting of formic acid (Fluka Chemie), DIPEA, *N*,*N*′-diisopropylcarbodiimide (DIPCDI, Aldrich), and TBTU (6:6:6:3) in DCM. The peptides were exposed for the mixture for 2 h during continuous stirring. The progress of the formylation process was followed by use of Kaiser test.[51] The resin was rinsed with DCM, and dried for 24 h. Cleavage of the peptides from the support and removal of protecting groups was achieved by a mixture of trifluoroacetic acid (TFA, Aldrich), ethanedithiol (EDT, Fluka Chemie), water, and triisopropylsilane (Aldrich) (94:2.5:2.5:1 v/v; 20 mL/g of polymer) for 2 h, with occasional stirring. The resin was rinsed with TFA and peptides separated by filtration. The TFA was evaporated, and the peptides were precipitated, washed, and pelleted in cold diethyl ether (Sigma-Aldrich). Pellets were resuspended in water and lyophilized. The peptides were purified with HPLC (ProStar, Varian Inc., Walnut Creek, CA) using a preparative C8 reversed phase column (Hichrom Ltd., Berkshire, U.K.). The short control peptide was eluted isocratically with 10% aqueous acetonitrile (ACN, Laboratory-Scan Analytical Sciences, Dublin, Ireland), whereas the long agonist was purified using a gradient of aqueous ACN from 80 to 50% in 20 min and from 50% to 30% in further 25 min and the short agonist using a gradient from 80% to 60% in 30 min. The purified peptides were stored in a lyophilized state. When used, the peptides were dissolved with the assumption that 30% of the total mass was water. During synthesis the products were continuously controlled by MALDI-TOF mass spectrometry (Voyager-DE STR Biospectrometry Workstation, Applied Biosystems). For some control experiments, commercially available FPR agonist fMLF (Sigma-Aldrich) and FPLR1 antagonist WRWWWW (Calbiochem, La Jolla, CA) were used. The latter was used at 1 μM, a dose reported to display no nonspecific activation in neutrophils.[52] In addition, the monoclonal azide free anti-CD11b antibody LM2/1.6.11 (a kind gift from Dr. Carl G. Gahmberg, University of Helsinki, Finland) was used to block adhesion and activation mediated by integrin CR3 (complement receptor type 3).[53]

Inorganic Supports. No. 1 Menzel-Gläser (Braunschweig, Germany) coverslips (30 × 0.17 mm) were evaporated with 10 Å titanium and 120 Å gold[30] for all microscopy studies. The coated slips were semitransparent (25−40% transmission) in the range 340−580 nm and thus compatible with examination using an inverted fluorescence microscope. Characterization of peptide immobilization using ellipsometry, contact angle goniometry, and infrared reflection−absorption spectroscopy (IRAS) was performed on standard, cleaned silicon (100) wafers (Wacker-Chemie GmbH, München, Germany) coated with a 25 Å titanium adhesion layer and, subsequently, with 2000 Å gold. Details on the substrate cleaning prior to deposition and the gold deposition can be found elsewhere,[54] with the exception that the evaporation rate for gold on the coverslips was reduced from 10 to 5 Å/s. Gold substrates were cleaned in a mixture of water, 30% hydrogen peroxide, and 25% ammonia (5:1:1) for 5 min at 80 °C and rinsed extensively in water prior to incubation.

Peptide Immobilizations. SAMs of hydroxyl- and maleimide-terminated EG_4 disulfides (Figure 1D,E) were used as linkers and spacers in the immobilization process, to offer extended flexibility,

(51) Kaiser, E.; Colescott, R. L.; Bossinger, C. D.; Cook, P. I. *Anal. Biochem.* **1970**, *34*(2), 595–598.

(52) Stenfeldt, A. L.; Karlsson, J.; Wennerås, C.; Bylund, J.; Fu, H.; Dahlgren, C. *Inflammation* **2007**, *30*(6), 224–229.

(53) Anderson, D. C.; Miller, L. J.; Schmalstieg, F. C.; Rothlein, R.; Springer, T. A. *J. Immunol.* **1986**, *137*(1), 15–27.

(54) Ekeroth, J.; Borgh, A.; Konradsson, P.; Liedberg, B. *J. Colloid Interface Sci.* **2002**, *254*(2), 322–330.

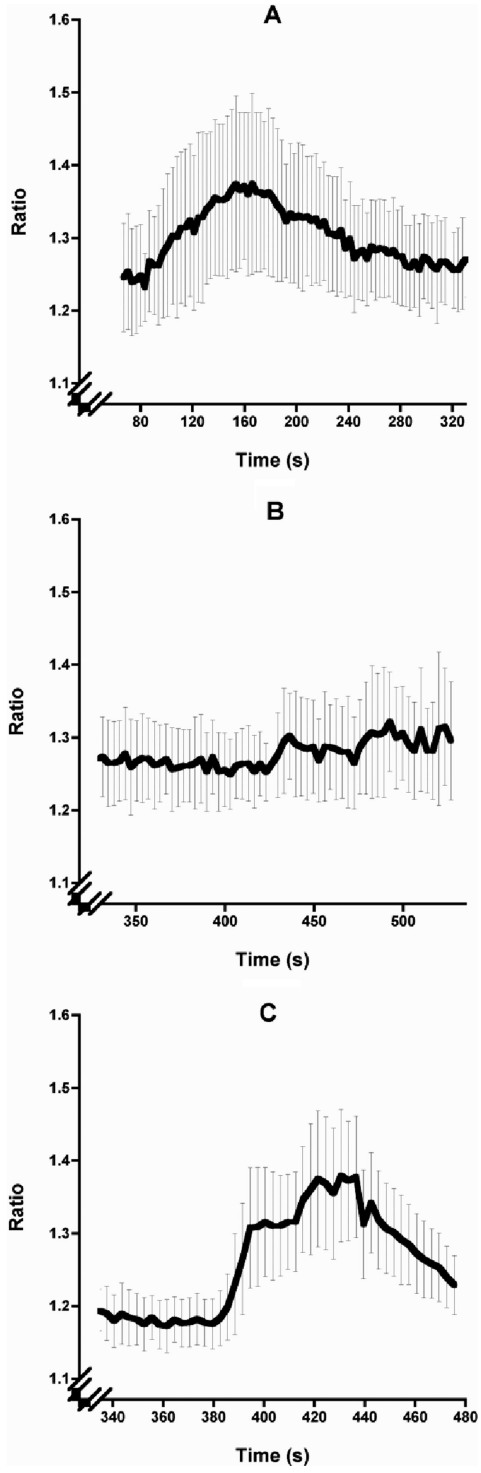

Figure 7. (A) The average cytosolic calcium response in 10 individual fura-2-loaded neutrophils during interaction with semitransparent gold-coated coverslips terminated with the long FPR agonist (at 100% maleimide termination). Experimental details essentially as in Figure 6, but image ratios acquired instead every third second. Bars denote the standard deviation. (B) The mean response of the very same cells in (A) subsequent to a humoral stimulation with 0.1 μM fMLF after 7 min (420 s). (C) The mean calcium response in 14 individual neutrophils in the focal plane of the formylated control peptide surface when stimulated with 0.1 μM fMLF after 6 min (360 s). (Please note the different scaling on the *x*-axes).

increasing the vertical distance, and shielding of the cells from the bare substrate. Cleaned substrates were incubated for 24 h in 50 μM solutions of maleimide- and hydroxyl-terminated EG_4 disulfides in ethanol (Kemetyl AB, Haninge, Sweden), with maleimide termination

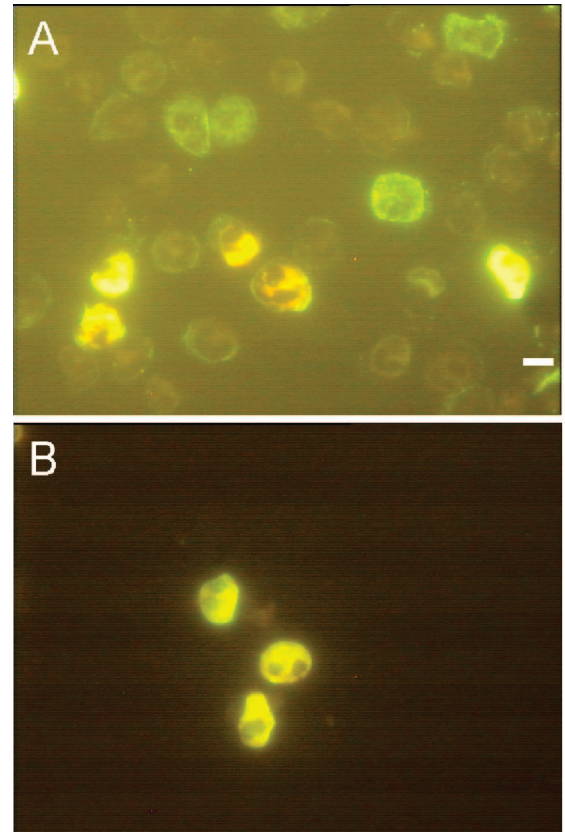

Figure 8. Human neutrophils loaded with fura-2 were exposed to surfaces for 15 min (as in Figure 6), paraformaldehyde-fixed, lysophophatidylcholine-permeabilized, and the filamentous actin cytoskeleton stained with Alexa488−phallacidin. Fluorescence microscopy revealed that the long agonist−peptide surface (A) rapidly recruited neutrophils to near full confluency over the entire matrix with cells displaying moderate to extensive spreading within a few minutes. The surface with the immobilized formylated control peptide surface (B) attracted only few scattered neutrophils that displayed low spreading. Note that (A) is representative for the typical cell count and morphologies observed on this coating but (B) is only representative for morphology since most views were actually entirely cell free. Photos shot with identical acquisition settings and editing kept to an absolute minimum, despite the relatively high distortion from the reflective gold layer. (Bar represents 10 μm.)

ranging from 10% to 100%. Peptide solutions (50 μM) were prepared in water (control peptide, Figure 1A), 50% ethanol (short agonist, Figure 1B), and dimethyl sulfoxide (long agonist, Figure 1C). Before analyses the surfaces coated with EG_4 disulfides or the short agonist were extensively rinsed in ethanol, ultrasonicated for 5 min, and blown dry with nitrogen gas. For the formylated control peptide ethanol was replaced by water and for the long agonist the rinsing and ultrasonication procedure was repeated twice, to ensure total removal of DMSO. Peptide coupling to the SAMs of maleimide- and hydroxyl-terminated EG_4 disulfides was accomplished by incubation of peptides (50 μM) in HBS-EP buffer (Biacore-GE Healthcare, Uppsala, Sweden) for 1 h. To enhance the solubility, the agonists were dissolved in a droplet of DMSO before adding HBS-EP. The surfaces were thoroughly rinsed in ethanol, ultrasonicated for 5 min, and dried with nitrogen before use. The samples were stored at room temperature in plastic Nalgene beakers precleaned by triplicate rinsing and 10 min ultrasonication in hexane and ethanol.

Neutrophilic Granulocytes (Neutrophils). Human neutrophils were isolated daily according to the methodology of Böyum and others following venipuncture of nonmedicated blood donors at the Linköping University Hospital.[55,56] Heparinized (5 IU/mL) whole

(55) Böyum, A. *Scand. J. Clin. Lab. Invest., Suppl.* **1968**, *97*, 77–89.
(56) Ferrante, A.; Thong, Y. H. *J. Immunol. Methods* **1980**, *36*(2), 109–117.

blood was layered on one part of Lymphoprep over four parts of Polymorphprep (Axis-Shield PoC AS, Oslo, Norway) in 50 mL test tubes and then centrifuged at room temperature for 40 min at 480*g*. The neutrophil fraction was harvested and washed in room tempered phosphate-buffered saline (PBS; 137 mM NaCl, 2.7 mM KCl, 6.7 mM $Na_2HPO_4 \times 2H_2O$ and 1.5 mM KH_2PO_4, pH 7.3) for 10 min at 480*g*, and the remaining red cells were eliminated by brief hypotonic lysis at 4 °C followed by washing (200*g* at 4 °C) in Krebs-Ringer phosphate buffer supplemented with glucose (10 mM) and $MgSO_4$ (1.5 mM), pH 7.3 (KRG). The cells were counted in a Coulter Counter ZM Channelyser 256 (Coulter-Electronics Ltd., Luton, U.K.). They were kept at 4 °C until prewarming to 37 °C and calcium reconstitution through the addition of $CaCl_2$ (1.1 mM) before the experiments. Imaging experiments were repeated independently with cells from two to three blood donors.

Ellipsometry. The thicknesses of the adsorbed layers were measured with an AutoEl III ellipsometer (Rudolf Research, NJ) equipped with a He−Ne laser light source ($\lambda = 6328$ Å) aligned at an angle of incident of 70°. The layer thicknesses were calculated using the McCrackin evaluation algorithm[57] and an optical three-layer model assuming isotropic and transparent layers with a refractive index of 1.5. Each sample was measured at five different points, and the number of surfaces was at least five.

Contact Angle Goniometry. The static contact angles with water were measured with a CAM 200 Optical Contact Angle Meter (KSV Instruments LTD, Helsinki, Finland). The needle (Hamilton Co., Reno, NV) was rinsed with a mixture of water, 25% hydrogen peroxide, and 30% ammonia (5:1:1) for 5 min at 80 °C and rinsed in water. Each sample was measured in one spot for which 10 images were recorded. For each sample at least five different surfaces were investigated.

Infrared Spectroscopy. The infrared experiments were performed in N_2-purged instruments to reduce the interference from water. Isotropic spectra of peptides dispersed in KBr were obtained with an IFS 48 system (Bruker Optics GmbH, Ettlingen, Germany) and the IRAS spectra were measured with a Bruker IFS 66 system equipped with a grazing angle (85°) infrared reflection accessory. Spectra were obtained by averaging 200 (KBr) and 3000 (IRAS) scans, respectively, at a resolution of 2 cm^{-1} and a three-term Blackmann−Harris apodization function was applied to the interferograms before Fourier transformation. A surface coated with deuterated hexadecanethiol ($HS(CD_2)_{15}CD_3$) was used for background and water vapor reference measurements.

Luminol-Dependent Chemiluminescence. The neutrophil generation of reactive oxygen species was studied with luminol-dependent chemiluminescence in a six-channel LB9505C Biolumat (Berthold Co., Wildbaden, Germany), essentially as described by Dahlgren and Karlsson.[58] Neutrophils were preincubated at least 5 min at 37 °C with horseradish peroxidase (4 IU/mL, Boehringer Mannheim GmbH, Mannheim, Germany) and luminol (56.4 μM, Sigma Chemical Co., St. Louis, MO). With this approach, both intra- and extracellulary oxygen intermediates are detected since luminol is membrane permeable and peroxidase is sufficiently available in both the intra- and extracellular compartment.

Ratio Imaging. Neutrophils were preloaded (5 μM) for 30 min at 37 °C with the fluorescent calcium-binding cell permeable acetoxymethyl derivate of fura-2 (5-oxazolecarboxylic acid, 2-(6-(bis(2-((acetyloxy)methoxy)-2-oxoethyl)amino)-5-(2-(2-(bis(2-((acetyloxy)methoxy)-2-oxoethyl)amino)-5-methylphenoxy)ethoxy)-2-benzofuranyl)-(acetyloxy)methyl ester, Molecular Probes-Invitrogen Corp., Carlsbad, CA), and washed twice in KRG. Then they were added to coverslip-bottomed 37 °C microscope stage chambers in KRG with Ca^{2+}, and immediately after cell sedimentation into the focal plane of the matrices (approximately 1 min after addition), the stage was fixed and the cells alternately excited at 340 and 380 nm, respectively. Emitted fluorescence was recorded at 510 nm, as averaged images every sixth second with a Photon Technology International, Inc. (Birmingham, NJ), ratio fluorescence imaging system. This was based on a Carl Zeiss (Jena, Germany) Axiovert 100 M with a 40× or 100×/1.3NA glycerol-immersion Neofluar objective. Cells were added to the solutions and immediately excitated at 340 and 380 nm, respectively, for every sixth second. The resulting ratio image is proportional to the calcium ion concentration.[34] Image acquisition and analysis were performed using the PTI ImageMaster (v. 1.4b8) software. To ascertain a cytosolic localization of the fluorescence, an additional camera (Hamamatsu C-2400, Hamamatsu Photonics K.K., Hamamatsu City, Japan) was used to capture bright field images at each time point by passing the transmission light through a 700 nm band-pass (100 nm) filter in front of the halogen lamp.

Fluorescence Microscopy. At the end of each ratio imaging session, i.e., 10 min after addition of cells, the samples were fixed for 30 min in ice-cold paraformaldehyde (4%) and washed twice in PBS. They were then permeabilized and stained for F-actin through incubation in lysophosphatidylcholine (100 μg/mL) and Alexa488- or Bodipy-phallacidin (0.6 μg/mL, Molecular Probes-Invitrogen) in PBS for 30 min at room temperature in darkness. The staining solution was removed by duplicate washings in PBS. The samples were mounted in ProLong Gold mounting medium (Molecular Probes-Invitrogen), and the cell morphology and adhesion were studied in a Zeiss Axioskop through 63×/1.4NA or 100×/1.3NA plan-apochromat oil objectives. Images were captured with a Carl Zeiss ZVS-47E digital camera using the Easy Image Measurement 2000 software (version 2.3, Tekno Optik AB, Solna, Sweden). Samples and controls were both acquired and edited (ImageJ software, version 1.33u, National Institutes of Health, Bethesda, MD) identically.

Acknowledgment. The Swedish Foundation for Strategic Research (Biomimetic Materials Science programme, *Biomics*), the Swedish Research Council, the Swedish Society for Medicine, the EU project *CellSens* (QLK3-CT-2001-00244), and the research foundations Goljes Minne, Magn. Bergvall, Lars Hiertas Minne, and Nanna Svartz are all acknowledged for financial support. Mr. Kenneth Abrahamsson and Dr. Johan Ekeroth are thanked for synthesis of the maleimide- and hydroxyl-terminated EG_4 disulfides, and Dr. Mattias Östblom is thanked for IR data processing.

Supporting Information Available: Table (S1) of ellipsometric thicknesses and contact angles for spontaneously adsorbed layers of control and agonist peptide analogues, as well as the SAMs of hydroxyl- and maleimide terminated EG_4 disulfides and figures of (S2) effects of blocking the integrin CR3 and FPLR-1 on neutrophil adhesion and morphology and (S3) fMLF-mediated inhibition of neutrophil spreading on the long agonist peptide surface. This information is available free of charge via the Internet at http://pubs.acs.org.

LA703502Y

(57) McCrackin, F. L. NBS Technical Note 479, **1969**.
(58) Dahlgren, C.; Karlsson, A. *J. Immunol. Methods* **1999**, *232*(1−2), 3–14.